Universitat de Girona

Facultat de Ciències

Memòria del Treball Final de Grau

DAPHNIA MAGNA RESPONSES TO ZERO-MEAN FLOW TURBULENCE.

Mara Franziska Müller

Grau en Biologia

maramuller88@gmail.com

Tutor: Jordi Colomer

Empresa / institució: Universitat de Girona

Vistiplau tutor:

Nom del tutor: Jordi Colomer

Empresa / institució: Universitat de Girona

Correu electrònic: jordi.colomer@udg.edu

Data de dipòsit de la memòria a secretaria de coordinació: 22/05/2018

INDEX

Page

ABSTRACT

Daphnia magna is a key zooplankton organism found in many freshwater aquatic systems. Its feeding usually includes phytoplankton as well as bacteria, but *Daphnia* are also able to feed on wastewater particles, which is why they have recently been considered as potential organisms for tertiary biologically based wastewater treatment. Even though *D. magna* is a well-studied species, little is known about the possible effect of the flow environment on its fitness. This study focuses on analysing the effect of zero mean turbulence on the filtration capacity, the swimming velocity and the 24h-survival of *D. magna* individuals with three different body lengths (L = 1.2, 1.5 and 1.8 mm). Results show a clear difference between the response to low or high turbulent shear rates. At low shear rates, *D. magna* individuals were able to swim more or less freely, especially the bigger ones, and the filtration rate increased, due to the greater *Daphnia*-particle encountering frequency. Hereafter, at low shears the swimming velocity of *D. magna* depended positively on the shear rate and negatively on the body length. On the other hand, at high shear rates *D. magna* individuals were not able to overcome the flow, thus presenting similar swimming speeds independent of the body length, and the filtration capacity was completely inhibited. The survival of the *D. magna* individuals followed the same trend, that is, at low shear rates individuals presented lower mortality than at high shear rates. However, smaller individuals showed to be more sensitive to the flow environment, as they presented higher mortality at low shear rates than the bigger individuals. In contrast, bigger *D. magna* individuals presented higher mortality at high shear rates, proving to be more vulnerable to high shears.

RESUM

Daphnia magna és un organisme zooplanctònic clau que es troba en molts sistemes aquàtics d'aigua dolça. La seva alimentació normalment inclou fitoplàncton i bacteris, però les *Daphnies* també són capaces d'alimentar-se de partícules d'aigües residuals, fet pel qual han estat recentment considerades com a potencials organismes per tractaments terciaris amb base biològica d'aigües residuals. Encara que *D. magna* sigui una espècie molt ben estudiada, se sap poc del possible efecte que pugui tenir la hidrodinàmica en la seva eficàcia biològica. Aquest estudi se centra en analitzar l'efecte de la turbulència d'un fluid amb cisallament (i amb velocitat global zero) en la capacitat de filtració, la velocitat de natació i la supervivència al cap de 24h d'individus de *D. magna* amb tres longituds corporals diferents (L = 1.2, 1.5 i 1.8 mm). Els resultats mostren una diferència clara en la resposta a baixes o elevades taxes de cisallament. A

baixes taxes de cisallament, els individus de *D. magna* eren capaços de nedar més o menys lliurement, especialment els més grans, i la taxa de filtració incrementava per causa de la major freqüència de trobada entre *Daphnies* i partícules. Així, a cisallaments baixos la velocitat de *D. magna* depenia positivament de la taxa de cisallament i negativament de la longitud corporal. Per contra, a elevades taxes de cisallament els individus de *D. magna* eren incapaços de superar el flux, presentant així velocitats de natació similars i independents de la longitud corporal, i la capacitat de filtració es trobava completament inhibida. La supervivència dels individus de *D. magna* seguia la mateixa tendència, és a dir, a baixes taxes de cisallament els individus presentaven menor mortalitat que a elevades taxes de cisallament. Tanmateix, els individus més petits resultaven ser més sensibles a la hidrodinàmica, ja que presentaven major mortalitat a baixes taxes de cisallament que els individus més grans. Per contra, els individus més grans de *D. magna* presentaven major mortalitat a altes taxes de cisallament, resultant ser més vulnerables a aquestes condicions.

RESUMEN

Daphnia magna es un organismo zoolplanctónico que se encuentra en muchos ecosistemas acuáticos de agua dulce. Su alimentación normalmente incluye fitoplancton y bacterias, pero las *Daphnias* también son capaces de alimentarse de partículas de aguas residuales, por lo que recientemente han sido consideradas como potenciales organismos para tratamientos terciarios con base biológica de aguas residuales. Aunque *D. magna* es una especie muy bien estudiada, se sabe poco del posible efecto de la hidrodinámica sobre su eficacia biológica. Este estudio se centra en analizar el efecto de la turbulencia de un flujo con cizallamiento (y con velocidad global cero) en la capacidad de filtración, la velocidad de natación y la supervivencia al cabo de 24h de individuos de *D. magna* con tres longitudes corporales distintas (L = 1.2, 1.5 y 1.8 mm). Los resultados muestran una clara diferencia entre la respuesta a bajas y elevadas tasas de cizallamiento. A bajas tasas de cizallamiento los individuos de *D. magna* eran capaces de nadar más o menos libremente, especialmente los individuos más grandes, y la tasa de filtración aumentaba, debido a la mayor frecuencia de encuentro entre *Daphnias* y partículas. Así, a cizallamientos bajos la velocidad de natación de *D. magna* dependía positivamente de la tasa de cizallamiento y negativamente de la longitud corporal. De lo contrario, a elevadas tasas de cizallamiento los individuos eran incapaces de superar el flujo, presentando así velocidades de natación similares e independientes de la longitud corporal, y la capacidad de filtración era completamente inhibida. La supervivencia de los individuos de *D. magna* seguía la misma tendencia, es decir, a bajas tasas de cizallamiento los individuos presentaban menores tasas de

mortalidad que a elevadas tasas de cizallamiento. No obstante, los individuos más pequeños mostraron ser más sensibles a la hidrodinámica, ya que presentaban mayor mortalidad a bajas tasas de cizallamiento que los individuos mayores. Por el contrario, los individuos más grandes de *D. magna* presentaban mayor mortalidad a elevadas tasas de cizallamiento, resultando ser más vulnerables a estas condiciones.

1. INTRODUCTION

One of the great challenges humanity is facing is the increasing need of secure freshwater resources, due to the exponential growth of its population. Adding the poor regulations of water use and the scarce policies for water demand, in 2016, 4 billion people experienced water scarcity in at least one month of each year (Mekonnen and Hoekstra, 2016).

Usually, the demands of reused and potable freshwater resources exceed the actual available supply of it. In addition, natural available ecosystems providing freshwater are confronting many direct or indirect anthropogenic pressures, such as climate change, pollution and overexploitation, so that the overall effect of these pressures results in threatening biodiversity, food security, economic growth and human well-being (Vollmer et al., 2018). For this reason, wastewater treatment plants (WWTP) are now viewed as future water resource recovery facilities, especially in water-deprived areas which are likely to experience increased water lack due to climate change (Serra and Colomer, 2016).

Water recycling and the quality of associated sewage effluents are usually controlled and should follow public water quality standards, in order to achieve safe health thresholds, as well as tolerable concentrations of suspended solids (Levine and Asano, 2004). However, most of the conventional tertiary systems in the WWTP are not able to remove small particles, such as microbes and fine suspended solids, that later promote poor water quality and increased levels of turbidity, respectively (Pau et al., 2013). Some tertiary treatments, such as ultrafiltration, ozonation and chlorination, are able to clarify and disinfect wastewater (Gómez et al., 2010), although not always being cost-effective and/or eco-friendly (Grant et al., 2012). A sustainable alternative to these conventional wastewater treatments are biologically based wastewater treatments, such as constructed wetlands, polishing ponds, high-rate algal ponds, and *Daphnia* and fungal reactors, which were found to be effective in the treatment of sewage as well as in removing emerging contaminants (Garcia-Rodríguez et al., 2014; Matamoros and Salvadó, 2012).

Daphnia magna is a key zooplankton organism found in many aquatic systems, which is easily cultured, shows rapid growth and has a constant genetic background with a clonal reproduction (Garreta-Lara et al., 2018). Its feeding usually includes phytoplankton as well as bacteria, and it is known to cause the so called clear water phase of a lake, known as the phase where the value of the phytoplankton population reaches the minimum. Studies of this phenomenon show that the phytoplankton bloom that occurs in a lake during spring is followed by a growth in *Daphnia*

populations grazing on the phytoplankton, making its populations decrease abruptly (Pau et al., 2013; Shiny et al., 2005; Straile, 2002, 2000).

Daphnia are able to feed on wastewater particles, which is why they have recently been considered potential organisms for tertiary biologically based wastewater treatment (Pau et al., 2013; Serra et al., 2014). In fact, Serra and Colomer (2016) demonstrated that *D. magna* was able to improve water quality of wastewater by decreasing the concentration of small particles, which are the most difficult to remove from sewage. Furthermore, *D. magna* has also been shown to remove emerging contaminants from wastewater (Garcia-Rodríguez et al., 2014; Matamoros and Salvadó, 2012) and to be sensitive to diverse products, which is the reason why it has been used as a model organism in ecotoxicology (Altshuler et al., 2011; Garreta-Lara et al., 2018). Besides, recent studies found that *D. magna* is capable of inducing local water mixing in stratified freshwater ecosystems if background turbulence is weak (Simoncelli et al., 2017), which poses a physical limit to be considered when *D. magna* is considered to be used as a filtration technology in mesocosmos (Serra and Colomer, 2016).

Many studies show the negative impact of unfavourable environmental conditions on the activity of *D. magna* (Maceda-Veiga et al., 2015; Pan et al., 2016). These unfavourable factors include high and low temperature (Garreta-Lara et al., 2018; Maceda-Veiga et al., 2015; Serra et al., 2014), high salinity (Garreta-Lara et al., 2018), high concentration of chemicals and drugs (Pan et al., 2016) and the presence of microplastics (Rehse et al., 2016), which produce disorders in the filtration capacity, swimming behaviour, growth, heartbeat, metabolism and survival of *D. magna* individuals (Bownik, 2017; Garreta-Lara et al., 2018).

Despite the fact that all these studies concern environmental factors, little is known about the possible effect of the flow environment on the filtration rate, the swimming characteristics and the survival of *D. magna*. Serra et al. (2018) studied the filtration efficiency and mobility of *D. magna* in laminar to turbulent shear flows. Even though the increase in the mean flow lead to an increase in the filtration capacity of *D. magna*, due to the increase in the particle-*Daphnia* encountering frequency, this positive effect was only found in the laminar flow regimes, characterized by shear rates of 0.18 to 3.15 s^{-1}. The filtration capacity of *D. magna* individuals in a laminar flow domain increased up to 2.6 ml ind^{-1} h^{-1} (for individuals with mean body length of 1.6 mm) and then dropped significantly when the flow regime turned from laminar to turbulent (with mean flows characterized by Reynolds numbers, Re > 1900), until it was completely inhibited, indicating that the *D. magna* individuals were unable to capture the particles in that domain. Serra et al. (2018), as well, proved that the swimming velocity of individuals of *D. magna*

increased in the laminar flow domain, with speeds of the individuals above the mean flow velocity. In the turbulent flow, *D. magna* individuals were dragged by the fluid and could not swim freely or faster than the flow.

Furthermore, previous studies (Burns, 1969a, 1969b) pointed out that the filtration rate of *D. magna* individuals positively depends on the body length with a power relationship of 3. The filtration rate has been proven to be a key parameter to characterize the fitness of *D. magna* individuals (Burns, 1969b, 1969a; Pau et al., 2013).

However, so far, no study has documented zero-mean flow turbulence effects on *D. magna* individuals. In this experimental design we exposed *D. magna* individuals to turbulent conditions as well as to control conditions. To characterize the fate of *D. magna* individuals in a sheared water domain, the designed protocol of experiments included measurements of *D. magna* individual characteristics, such as the swimming velocities, the 24h-lethal/sublethal response and the filtration capacity. The experiments were characterized by low shears, with shear rates of 1.1 – 11.8 s^{-1}, corresponding to turbulent kinetic energy dissipations expanding from 1.24×10^{-6} to 1.82×10^{-4} W/kg.

2. OBJECTIVES

This study is aimed to:

(1) The experimental analysis of the response of *D. magna* individuals to a sheared flow domain, with the response being determined by the effects of the turbulent flow on three parameters that characterize *D. magna* individuals: the swimming velocities, the 24h-lethal/sublethal response and the filtration capacity.

(2) The definition of a canonical model to predict the fate of *D. magna* individuals, in the range of shears where particle filtration by *D. magna* individuals is maximised.

3. CONTEXTUALIZATION OF THE STUDY

This study is set to gain knowledge on the experimental characteristics in which the capacity of *D. magna* filtration is maximised. The results obtained in this study will help to fulfil the objectives of an international project, the INNOQUA project, aimed to provide an ecological water sanitation system for rural areas and communities, for industries with specific

characteristics (such as agriculture and aquaculture), for sustainable home-builders or collective housing owners and for developing countries worldwide. This study is designed to set the best hydrodynamic experimental conditions *D. magna* individuals may encounter in a reactor or filter system, *i.e*, the range of internal dynamic working conditions that a reactor or filter system should attain, where *D. magna* individuals will thrive in order to increase the effluent water by both reducing the level of the turbidity and the concentration of microbial communities.

4. MATERIALS AND METHODS

4.1. The oscillating grid system

The basis of this study was an oscillating grid system (Fig. 1 and Fig. 2). similar to that described in Colomer et al. (2005) and Peters and Gross (1994). It consisted of three grid shafts hold by a frame attached to a controlled motor that provided up and down movement. Thus, three replicate containers could be used. The height of the Plexiglas containers was h = 19 cm and the radius r = 7.51 cm. Each container was filled with water up to h_w = 18 cm. Therefore, the working volume of each container was of 2.89 l.

Fig. 2. Image of one of the three Plexiglas containers used for the experiments along with the oscillating grid.

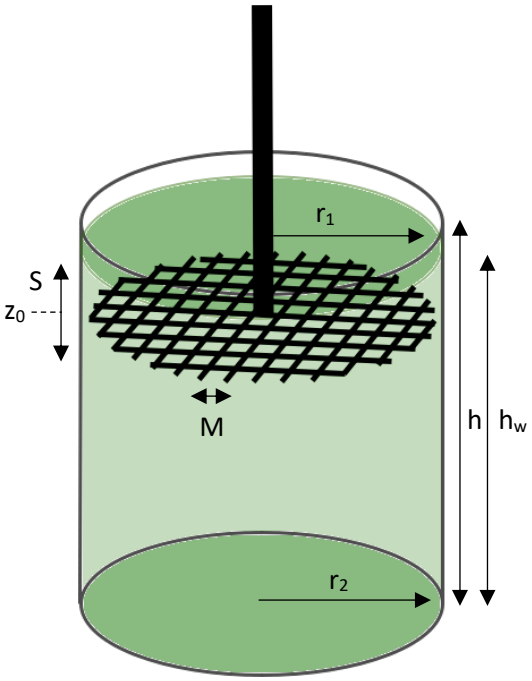

Fig. 1. Scheme of the experimental set-up for the oscillating grid system device. r_1 is the radius of the grid, r_2 is the radius of the Plexiglas container, h is the height of the Plexiglas container, h_w is the water height, S is the stroke, z_0 is the virtual origin and M is the mesh size.

The oscillating frequencies of the grids inside the Plexiglas containers ranged from 0.5 to 2.3 Hz (Table 1) with an oscillating amplitude (stroke, S) of 5 cm. The material of the grids was cylindrical stainless steel coated with a plastic polyamide, with a radius of 0.4 cm and a mesh size (M) of 1.5 cm. Solidity, which is the percentage of solid surface, in this case the surface of the grids, perpendicular to the direction of movement, was 40.2%, similar to that of 37.8 % used by Guadayol et al. (2009). With this set-up, the oscillating grids were always switched on with the grids situated at its mid position, defined here as the virtual origin (z_0), 3 cm from the working height cylinder (h_w), and 2.5 cm from the highest and lowest point of the oscillation amplitude. The rectilinear oscillating motion of the grid was ensured by constraining the connecting grid shafts to move along a guide rail using precision bearings (De Silva and Fernando, 1994). In order to avoid secondary circulation in the tank, the grid was designed such that the distance between the end of the grid and the wall of the cylinder was equal to half a square of the grid (Serra et al., 2008).

Table 2. Data corresponding to the experimental conditions of each run. The frequency values correspond to those obtained during the calibration of the oscillation grid, u', v' and w' are the RMS velocities in the three directions (x, y, z), k is the turbulent kinetic energy, ε is the dissipation rate of the fluid calculated from Eq. (4), G is the mean shear rate in the container, Re is the Reynolds number of the grids calculated from Eq. (9) and λ is the size of the smallest turbulent eddies within the fluid estimated from the Kolmogorov length scale with Eq. (10).

Frequency (Hz)	u' = v'	w'	k	ε ($m^2 s^{-3}$)	G (s^{-1})	Re_G	λ (mm)
0.5	0.0008	0.0009	3.59E-06	1.24E-06	1.1	15	0.93
0.6	0.0009	0.0011	4.93E-06	2.00E-06	1.4	17	0.83
0.7	0.0012	0.0014	8.26E-06	4.34E-06	2.1	23	0.68
0.9	0.0015	0.0016	1.15E-05	7.16E-06	2.7	27	0.60
1.0	0.0017	0.0019	1.54E-05	1.10E-05	3.4	31	0.54
1.1	0.0019	0.0021	1.95E-05	1.58E-05	4.0	35	0.49
1.3	0.0021	0.0024	2.40E-05	2.15E-05	4.7	38	0.46
1.4	0.0023	0.0026	2.92E-05	2.88E-05	5.4	42	0.42
1.5	0.0025	0.0029	3.56E-05	3.88E-05	6.3	47	0.39
1.6	0.0028	0.0031	4.15E-05	4.89E-05	7.1	51	0.37
1.8	0.0030	0.0034	4.79E-05	6.07E-05	7.9	54	0.35
1.9	0.0032	0.0036	5.64E-05	7.75E-05	8.9	59	0.33
2.0	0.0034	0.0039	6.39E-05	9.33E-05	9.8	63	0.32
2.2	0.0036	0.0041	7.14E-05	1.10E-04	10.6	66	0.30
2.3	0.0039	0.0044	8.25E-05	1.37E-04	11.8	71	0.29

4.2. The fundamental theory of grid turbulence

The fundamental theory of the oscillating grid system devices focuses either on the vertical distribution of turbulent kinetic energy (Orlins and Gulliver, 2003) or on the mean turbulent kinetic energy dissipation rate, ε (Colomer et al., 2005; Huppert et al., 1995; Pujol et al., 2010; Serra et al., 2008). The bulk turbulent kinetic energy dissipation in the tank is related to the mean shear rate, G. The parameter G has been widely used to describe the aggregation of particles by the oscillating grid devices under high turbulence (Serra et al., 2008) and also in low-shear flows (Colomer et al., 2005).

The main contributions to the study of the grid turbulence devices are Hopfinger and Toly (1976), Rouse and Dodu (1955), Thompson and Turner (1975) and Xuequan and Hopfinger (1986). They described the fundamental theory of the grid turbulence devices which is characterized by its zero-mean flow, and by being two-dimensionally homogeneous in a certain region away from the grid. The horizontal and vertical root-mean square turbulence velocities (u' and w') decay linearly with depth while the integral length scale increases with distance z in the form:

$$u' = v' = C_1 M^{0.5} S^{1.5} f z^{-1} \text{ and } w' = C_2 M^{0.5} S^{1.5} f z^{-1} \quad (1)$$

where u', v', and w' are the RMS velocities in the three directions (x, y, z), respectively; M is the mesh size (defined as the distance between centres of two grid bars); C_1 = 0.22, C_2 = 0.25 and C_3 = 0.10 are constants depending on the grid geometry (De Silva and Fernando, 1994). Besides, the turbulent kinetic energy decreases according to $k \propto z^{-2}$, and the Reynolds number remains nearly constant during the decay. The turbulent kinetic energy defined as

$$k = (u'^2 + v'^2 + w'^2)/2 \quad (2)$$

can then be expressed as

$$k = \frac{1}{2}(2C_1^2 + C_2^2)(M^{0.5} S^{1.5} f z^{-1}) \quad (3)$$

while the average energy dissipation rate ε and the shear rate G, are expressed as

$$\varepsilon = \gamma u'^3 l \quad (4)$$

$$l = C_3 z \quad (5)$$

$$G = (\varepsilon/\nu)^{1/2} \quad (6)$$

where γ is a constant taken equal to 0.8, l is the integrand length scale with distance from the grid, u' is the integral velocity and ν = 10^{-6} m^2 s^{-1} is the kinematic viscosity of the flow at 20 °C. Using equations (1), (4) and (6) it is possible to obtain the dependence of the shear rate on the grid characteristics, the frequency of the grid and the depth, according to

$$G = \sqrt{\frac{\gamma}{\nu C_3} C_2^3 \frac{M^{3/2} S^{9/2} f^3}{z^4}} \quad (7)$$

which considering the values of the parameters, and a mesh size of 1.5 cm may be reduced to

$$G = 0.01811 f^{3/2} z^{-2} \quad (8)$$

The mean shear rate in the containers may be calculated taking the average of G by integrating G over the depth from z = z_o to the working height (Table 1). For the frequencies and the working height, G was found to be in the range of 1.1 to 11.8 s^{-1}, therefore in the range of low shear flow (Colomer et al., 2005). The Reynolds number of the grid can be calculated with $Re_G = u' l/\nu$ and Equations (1) and (5), as follows

$$Re_G = \frac{C_1 C_3 M^{0.5} S^{1.5} f}{\nu} \quad (9)$$

which is independent of the distance from the grid. The Re_G ranged from 15 to 71 depending on the value of *f*, corresponding in all cases to the turbulent regime. Finally, the size of the smallest turbulent eddies within the fluid was estimated from the Kolmogorov length scale λ according to

$$\lambda = (\nu^3/\varepsilon)^{1/4} = (\nu/G)^{1/2} \quad (10)$$

The Kolmogorov length scale was found to vary from 0.93 to 0.29 mm, being smaller than the *Daphnia magna* individual sizes.

4.3. Calibration of the oscillation grid

Each of the three Plexiglas containers were filled with 2.89 l bottled mineral water without spirulina suspension. The oscillations of the grid were counted at 20 different voltages for one minute three times, obtaining the corresponding frequencies (oscillations s^{-1}) represented in Fig. 3 with the letter *f*.

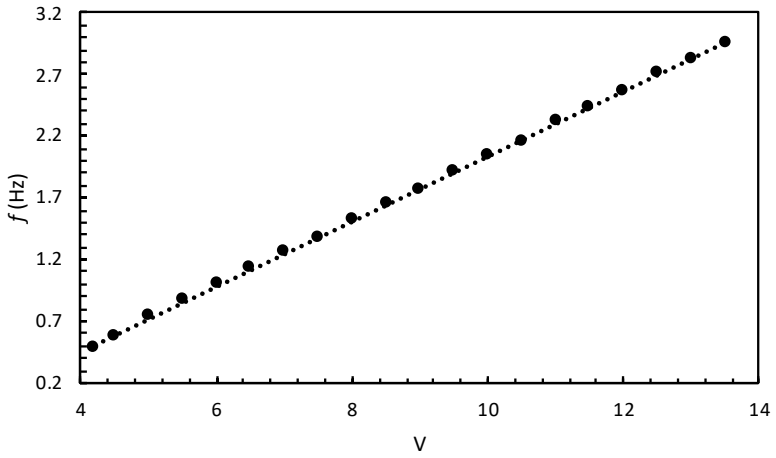

Fig. 3. Oscillating frequency (Hz) of the grids plotted versus voltage (V). The equation corresponding to the linear best fit (dashed line) is f = 0.26V – 0.59, with R^2 = 1.00.

4.4. Experimental method

Each experiment was carried out in a Plexiglas container filled with bottled mineral water and spirulina suspension, achieving a final concentration of 50 ml spirulina suspension l^{-1} and a final volume of 2.89 l per container. To prepare the spirulina suspension, 1 g of spirulina powder was diluted in 1 l bottled mineral water, mixed for 60 s at 100 rpm and left for 1 h in order to let large spirulina particles settle. The supernatant was used as the spirulina suspension for the experiments. Pau et al. (2013) showed that the particle concentration by the ingestion of *Daphnia magna* decreased exponentially. They chose the time t at which the initial concentration decreased in e^{-1} = 0.37 as the characteristic time in all the experiments, which was approximately of 4 hours. Therefore, all experiments were run for four hours.

Experiments began at a shear rate of 0 s^{-1} followed by controlled shear rates between 1.1 and 11.8 s^{-1}. The experiments executed at a shear rate of 0 s^{-1} were characterized by lacking induced mixing by the grids. Thus, at 0 s^{-1} there was only sedimentation of the spirulina particles, while at shears between 1.1 and 11.8 s^{-1} there was a combination of both the sedimentation of spirulina particles and the induced mixing by the grids on the containers. The shearless experiment without *D. magna* showed that c/c_0 after 4 hours was 0.54, indicating that sedimentation contributed to a 46% of particle removal. For control experiments with shear, c/c_0 varied from 0.57 at G = 1.1 s^{-1} to 0.61 at G = 11.8 s^{-1}, indicating that sedimentation was reduced in a range of 43 % and 39 %, respectively.

The spirulina particle size distribution in the suspension of the experiments was measured with a laser particle size analyser, the Lisst-100x (Sequoia Inc.). The Lisst instruments consist of multi-parameter measurements through the scattering at a set of multiple angles. The particles are illuminated by a laser beam formed by collimating the output of a diode laser. The focal plane of a receiving lens detects the scattering by particles. To distinguish the particle size, logarithmically distributed in the range of 2.5 – 500 μm, a detector consisting of 32 rings is placed in the focal plane. Each ring measures the scattering at a particular small range of angles and this energy distribution sensed by the ring detector is recorded by the Lisst instrument. After the data collection is completed, the data are offloaded and mathematically inverted to obtain the size distribution by means of the absolute volume concentration of each particle size. To do the measurement, a sample volume of 80 ml is needed. Therefore, 40 ml of sample were diluted with 40 ml of bottled mineral water. Particle concentration was calculated by integrating the concentration of the particles within the *Daphnia magna* feeding range, from particles of 2.5 to 30 μm in diameter. Therefore, the volume concentration of particles within the range of 2.5 to 30 μm was used to evaluate particle removal. It has been proven that the analyser shows good performance in determining particle size distribution and concentration for both organic and inorganic particles (Serra et al., 2002a, 2002b, 2001) in water suspensions.

4.5. *D. magna* characteristics

Individuals of *D. magna* were collected from a laboratory culture maintained at the facilities of the University of Girona in a 40 l container at 20 ± 0.5 °C and natural daylight photoperiod. Continuous air supply kept the water container oxygenated. Individuals were fed twice a week with a mixture of commercial spirulina powder and baker's yeast (*Saccharomyces cerevisiae*). Thirty percent of the water from the container was renewed once every fifteen days.

Thirty-three experiments were carried out with *Daphnia magna* individuals, at a concentration of 50 individuals l^{-1}. Pau et al. (2013) and Serra and Colomer (2016) found that at a *D. magna* concentration of 50 individuals l^{-1} the particle removal efficiency in laboratory conditions over 12 h was about 30 %, therefore proving to be the minimal concentration needed to ensure enough particle removal. *D. magna* individuals were distributed depending on their size. 11 experiments were carried out with *D. magna* individuals presenting a mean size of 1.2 ± 0.2 mm, 11 experiments with *D. magna* individuals presenting a mean body length of 1.5 ± 0.2 mm, and 11 more experiments with *D. magna* individuals 1.8 ± 0.2 mm long. To collect small size individuals two meshes were used; the first one with 1 mm spacing in order to discard retained

individuals larger than 1 mm and the second one with 0.5 mm spacing in order to collect retained individuals of 1 mm and discard the smaller ones. Mid-size *D. magna* individuals were collected from the cultures with a mesh of 1 mm spacing in order to discard individuals smaller than 1 mm. Larger individuals were separated in a second container and allowed to grow to obtain the biggest individuals. The mean size of the *D. magna* individuals was obtained by using the ImageJ software from a video recording of 10 individuals during each set of experiments.

Measures were done at t_0 (before turning on the oscillation grid system) and at t_4, for each of the thirty-three experiments. Furthermore, another measurement was done at t_{24}, in order to carry out the *D. magna* death evaluation.

4.6. Control experiments

Twelve control experiments were carried out under different *f* obtained during the calibration, each of them without *D. magna* individuals to study the particle removal by sedimentation. Measures were done at t_0 (before turning on the oscillation grid system) and at t_4, for each of the fifteen frequencies. Furthermore, some measurements were done at t_{24}, in order to make sure that enough feeding particles remained for the ingestion of *D. magna*.

4.7. *D. magna* velocity

The *D. magna* velocity was analysed by video recording the movement of the *D. magna* individuals, following (Serra et al., 2018). The camera recorded 25 frames per second and the *D. magna* trails were recorded for 1 min for each case, giving a total of 1500 frames. These frames were analysed with ImageJ software using the Mtrack plugin, according to Pan et al. (2016) and Moison et al. (2012). At each time step, the positions in the x (horizontal) and y (vertical) axis were analysed and the velocities in the x and y directions calculated. In each case, ten *D. magna* individuals were considered and a mean value for the velocities was calculated. The x and y component of the velocity was calculated from the temporal evolution of the (x, y) positions of each *D. magna* individual at each time step. The mean *D. magna* speed was calculated as:

$$v_{Dph} = \sqrt{\bar{v}_x^2 + \bar{v}_y^2} \tag{11}$$

where v_x and v_y are the mean velocities of all the trails in the x and y axis, respectively.

Furthermore, previous studies (Huntley and Zhou, 2004; Kunze, 2011) have examined the relationship between hydrodynamics of swimming and the body size of different marine species.

Kunze (2011) converted these relationships to functions of body size for two different types of swimming velocities, cruising (u_c) and escape (u_e), obtaining the following equations: $u_c = 3.23L^{0.83}$ and $u_e = 7.76L^{0.53}$, where L is the body length. Later, Wickramarathna et al. (2014) observed that the swimming velocities of *D. magna* closely followed the relationship for cruising speed, as escape behaviour was not observed in their study. Hereafter, swimming velocity of *D. magna* was analysed with the ImageJ software for three different mean body lengths (L = 1.2, 1.5 and 1.8 mm) under steady flow conditions (G = 0 s^{-1}), as well as under different shear rates (1.1 - 11.8 s^{-1}).

4.8. *D. magna* filtration capacity

Samples from each Plexiglas container were taken at two different times (t_0 and t_4) and spirulina particle size distribution in the suspension was measured with the Lisst-100x particle size analyser (Sequoia Inc.). Since the temporal evolution of the suspended particle concentration decreased exponentially, the concentration may be described by an exponential decay equation as follows (Pau et al., 2013):

$$c = c_0 e^{-kt} \tag{12}$$

where k is the rate of particle removal by both sedimentation (k_s) and *D. magna* filtration (k_{Dph}), i.e. $k = k_s + k_{Dph}$. From Eq. (12), k can be solved following

$$k = -\frac{1}{t}\ln\left(\frac{c}{c_0}\right) \tag{13}$$

and k_s can be determined from those experiments without individuals of *D. magna* (in which $k_{Dph} = 0$). Therefore, k_{Dph} will be calculated for the rest of the experiments. The rate of decrease due to *D. magna* filtration is a function of the filtering rate of each *D. magna* individual (F, in ml ind^{-1} l^{-1}) and the *D. magna* concentration in such a way that (Pau et al., 2013):

$$k_{Dph} = F\ x\ C_{Dph} \tag{14}$$

Furthermore, Burns (1969b) studied the relation between filtering rate, temperature and body size of four *Daphnia* species and found a clear dependence of the filtering rate on the body length. He pointed out that at 20 °C, the filtering rate could be described as $F = 0.208L_b^{2.8}$, where F is the filtering rate (ml $animal^{-1}$ h^{-1}) and L_b is the body length in mm.

4.9. *D. magna* filtration versus the shear rate

Li and Logan (1997) studied the particle collision rates in a turbulent shear environment between two populations consisting of fractal aggregates and small particles. In this study, the two populations are *D. magna* and small suspended spirulina particles. Since the Kolmogorov length scale was found to be smaller than the *D. magna* individual sizes, the rate of small particles captured by a single *D. magna* individual R_{Dph} can be written as (Kiørboe and Saiz, 1995)

$$R_{Dph} = \alpha G^{2/3} L^{7/3} c + R(0) \tag{15}$$

where α is the capture efficiency for each *D. magna* individual, G is the shear rate, L is the *D. magna* length-scale and $R(0) = k_{Dph}(0)\, x\, c$ is the particle removal by each *D. magna* individual in a steady flow (G = 0 s^{-1}). Therefore, the rate of the decease of small suspended particles due to *D. magna* feeding can be written as

$$\frac{1}{c_{Dph}} \frac{dc}{dt} = -\alpha G^{2/3} L^{7/3} c - \frac{R(0)}{c_{Dph}} \tag{16}$$

and merging Eqs. (12) and (16) results in

$$-\frac{c_0}{c_{Dph}} k_{Dph}(G) e^{-c_{Dph(G)t}} = -\alpha G^{2/3} L^{7/3} c \frac{k_{Dph}(0) c}{c_{Dph}} \tag{17}$$

and with Eq. (12)

$$\frac{k_{Dph}(G)}{c_{Dph}} = \alpha G^{2/3} L^{7/3} + \frac{k_{Dph}(0)}{c_{Dph}} \tag{18}$$

and therefore

$$k_{Dph}(G) = \alpha c_{Dph} G^{2/3} L^{7/3} + k_{Dph}(0). \tag{19}$$

Using Eqs. (14) and (19) the filtration F is function of G, α and L, that can be written as

$$F = \alpha G^{2/3} L^{7/3} + F(0) \tag{20}$$

Where $F(0) = k_{Dph}(0)/c_{Dph}$.

4.10. Uncertainty analysis

In order to add error bars to the various graphics, propagation of error was carried out using the following general simplified formula (Ku, 1966)

$$s_f = \sqrt{\left(\frac{\partial f}{\partial \mathrm{x}}\right)^2 s_x^2 + \left(\frac{\partial f}{\partial \mathrm{y}}\right)^2 s_y^2 + \left(\frac{\partial f}{\partial \mathrm{z}}\right)^2 s_z^2 + \cdots} \tag{21}$$

where s_f represents the standard deviation of the function f, s_x represents the standard deviation of x, s_y represents the standard deviation of y, and so on.

5. RESULTS

5.1. *D. magna* swimming velocity

The average instantaneous speeds of *D. magna* individuals at different shear rates were calculated from v_x and v_y following Eq. (11) for three different mean diameters (d = 1.2, 1.5 and 1.8 mm) and are represented in Fig. 4. When the flow was at rest, the mean swimming speed was 5 ± 2 cm s^{-1} for the smallest individuals (d = 1.2 mm), 7 ± 3 cm s^{-1} for the mid-sized individuals (d = 1.5 mm) and 9 ± 4 cm s^{-1} for the biggest ones (d = 1.8 mm). Once the flow turned turbulent, the average velocity of the 1.2 mm long *D. magna* individuals increased rapidly up to 11 ± 5 cm s^{-1} at a mean shear rate of 1.1 s^{-1} and then kept rising significantly along with the increase of the shear rate. On the contrary, the 1.8 mm long individuals were more resistant to the water flow, thus showing a much slighter increase in the swimming velocity at low shear rates. Therefore, the average speed of these individuals soon became the lowest one, although starting with the highest value. This resistance to being dragged was maintained until mean shears of 4.7 s^{-1}, from where the flow started dominating their speed, just like the other *D. magna* sizes. Finally, the

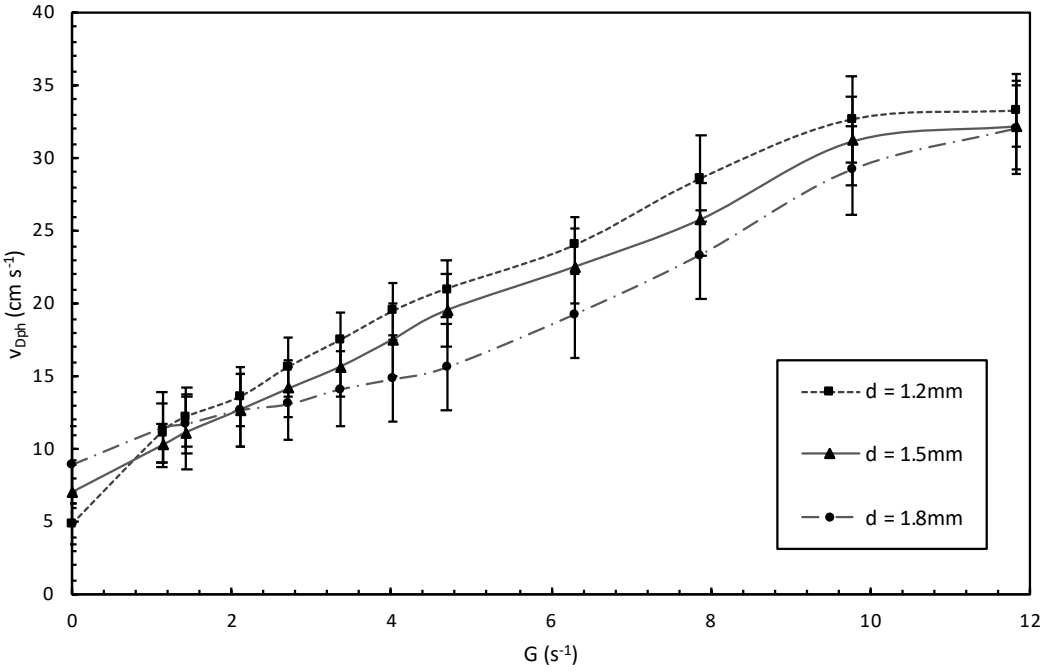

Fig. 4. Mean instantaneous speed of *D. magna* individuals (v_{Dph} in cm s^{-1}), calculated with Eq. (11), plotted versus the mean shear rate (G in s^{-1}) for four different *D. magna* lengths (L = 1.2, 1.5 and 1.8 mm).

mid-sized individuals (d = 1.5 mm) showed an intermediate trend between the other two sizes, being also rapidly dragged by the flow. However, at shear rates above 9.8 s^{-1} there was no longer a significant increase in the mean swimming velocity of the *D. magna* individuals and the values for the three different sizes became very similar, around 32 $\pm$ 15 cm s^{-1}. Hereafter, there is a differentiated regime at low shear rates and high shear rates. The transition from one regime to the other depends on the *D. magna* body length, so that the low shear rate regime comprises the following shears: G = 0 – 2.1 s^{-1} for *D. magna* individuals with d = 1.2 mm, G = 0 – 2.7 s^{-1} for a mean body length of 1.5 mm and G = 0 – 4.7 s^{-1} for 1.8 mm long individuals.

In order to find a function relating the mean *D. magna* velocity to the values of G (shear rate) and L (*D. magna* body length), a dimensionless analysis was carried out by plotting the dependence of velocity scales $^{v_{Dph}}/_{LG}$ versus the Reynolds number of the *D. magna* individuals. This analysis was done by separating the low shear rate regime from the high shear rate regime, following the classification mentioned earlier (G = 0 – 2.1 s^{-1} for d = 1.2 mm, G = 0 – 2.7 s^{-1} for d = 1.5 mm and G = 0 – 4.7 s^{-1} for d = 1.8 mm) (Fig. 5). The results of this analysis show that there is a different influence of the shear rate and the body length of *D. magna* on the swimming velocity, depending on whether it is the low shear rate regime or the high shear

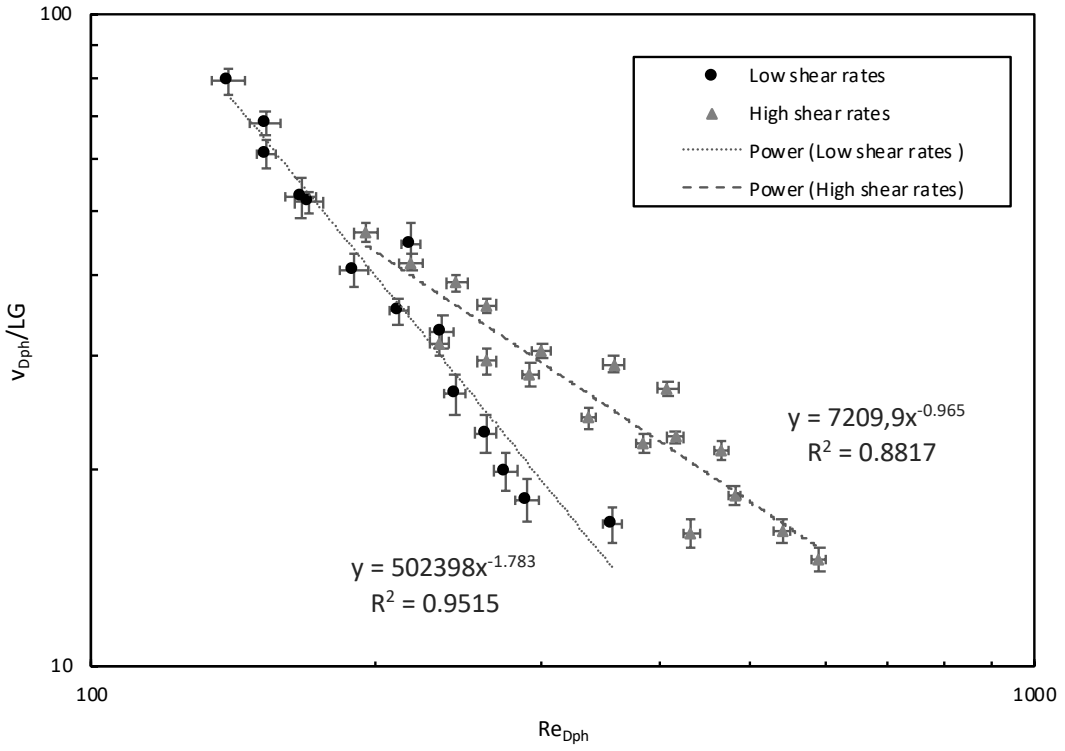

Fig. 5. Dimensionless analyses for the *D. magna* Reynolds (Re_{Dph}) and the dependence of velocity scales $^{v_{Dph}}/_{LG}$, where v is the mean swimming velocity, L is the mean body length and G is the shear rate. The two dashed lines show the power trendline with its corresponding equation and R-squared value.

rate regime. Both power relationships show a confidence level of 99%. For low shear rates, the relation between the three parameters can be expressed as

$$v_{Dph} = G^{0.36} c_1 \nu^{0.64} L^{-0.28} \quad (22)$$

where c_1 is a constant equal to 111.8, $\nu = 10^{-6}$ m^2 s^{-1} is the kinematic viscosity of the flow at 20 °C and L is the *D. magna* mean body length. Hereafter, the shear rate has a positive effect on the swimming speed of *D. magna*, while the body length influences negatively. In contrast, for high shear rates the resulting equation would be

$$v_{Dph} = c_2 \sqrt{\nu G} \quad (23)$$

where c_2 is a constant equal to 84.9. Unlike the previous case, at high shear rates the body length has no influence at all on the swimming velocities of the individuals.

5.2. Temporal evolution of the particle removal

Fig. 6 and 7 show the particle volume concentration of the suspension with spirulina for the particles in the range of 2.5 – 500 μm in diameter, measured at t = 0 h and t = 4 h for the experiments carried out at G = 1.1 s^{-1} (Fig. 6) and G = 7.9 s^{-1} (Fig. 7). The figures represent the control conditions (Fig. 6a and Fig. 7a) as well as the experimental conditions carried out with *D. magna* individuals, with body lengths of 1.2 mm (Fig. 6b and Fig. 7b), 1.5 mm (Fig. 6c and Fig. 7c) and 1.8 mm (Fig. 6d and Fig. 7d). A decrease in the total particle volume concentration with time is observed in the control experiments at both shear rates, due to particle sedimentation. However, at higher shear rates the decrease of bigger particles is much lower in comparison to mid-particles (d ≈ 10 – 40 μm), confirming that the shear produced at higher oscillation frequencies causes particle aggregation. Plus, this decline in the decrease of bigger particles is also promoted by the mixing induced by the grids. As for the experiments with *D. magna* (Fig. 6b, 6c, 6d, 7b, 7c and 7d), a shear rate of 1.1 s^{-1} (Fig. 6) favours the ingestion of particles smaller than 30 μm in diameter by *D. magna* individuals, thus increasing the difference between the initial (t = 0 h) and the final concentration (t = 4 h) of particles in the mentioned range. This particle volume concentration difference of particles within the *D. magna* feeding range increases along with the increase in the mean body length. On the other hand, a G of 7.9 s^{-1} inhibits the filtering capacity of *D. magna*, which is why a significant reduction of the particles within the ingestion range of the crustacean (2.5 to 30 μm in diameter) is no longer observed.

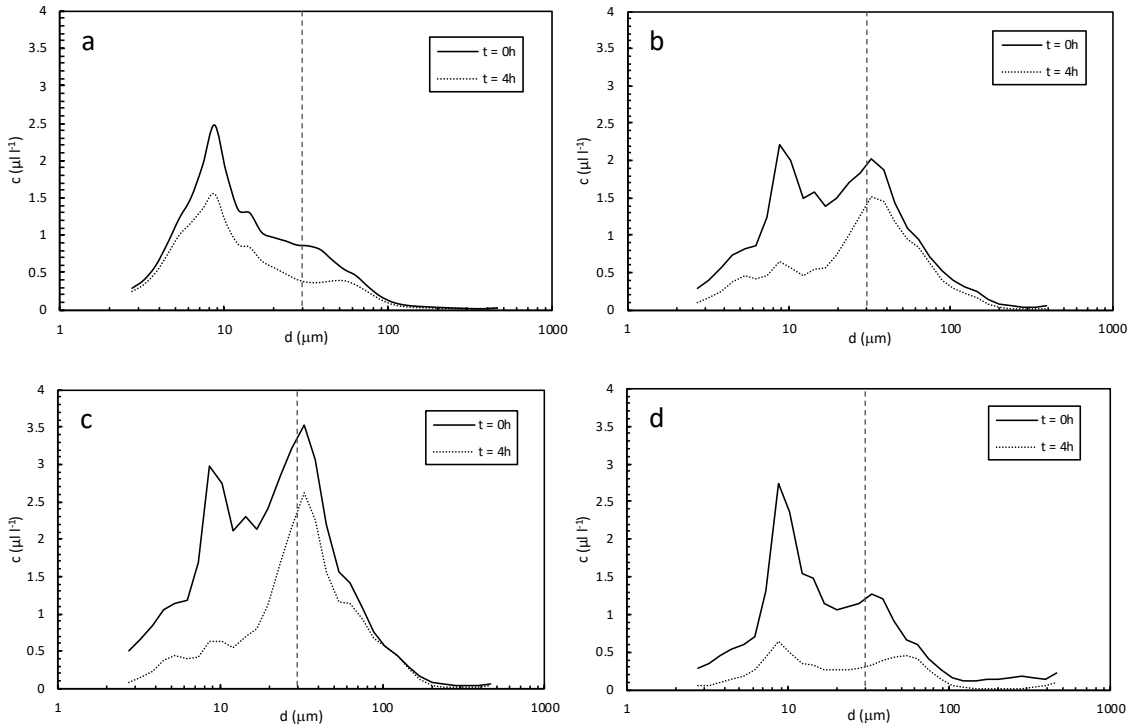

Fig. 6. Particle size distribution for the case of experiments carried out at G = 1.1 s^{-1} for two time steps, initially (t = 0 h) and after 4 h of treatment (t = 4 h). (a) corresponds to the control experiment carried out without *D. magna* individuals and (b), (c) and (d) correspond to the experiments carried out with *D. magna* individuals with body lengths of 1.2, 1.5 and 1.8 mm, respectively. The dashed vertical line corresponds to the limit of the ingestion particle size by *D. magna* individuals. In the vertical axis, the particle volume concentration in µl l^{-1} is represented and in the x-axis the diameter of the suspended particles in µm with logarithmic scale. Samples were diluted with bottled mineral water with a dilution factor of 1:1.

The ratio of c/c_0 calculated for the control experiments and for the experiments with *D. magna* individuals of three different mean diameters (d = 1.2, 1.5 and 1.8 mm) versus the mean shear rate (G) is plotted in Fig. 8. For the control experiments, c/c_0 at rest (G = 0 s^{-1}) was 0.54 and rapidly increased at mean shear rates ≥ 1.1 s^{-1}, reaching a value of ≈ 0.57. This digit remained constant up to mean shear rates of 6.3 s^{-1}, increasing significantly afterwards up to 0.61 for a mean shear rate of 11.8 s^{-1}. This significant rise coincides with the G values corresponding to the transition from laminar to turbulent flow found by Hinze (1975). For the experiments with individuals of *D. magna*, c/c_0 at rest was 0.47 for a mean body length of 1.2 mm, 0.39 for a body length of 1.5 mm and 0.30 for a mean body length of 1.8 mm. For the experiments run with the smallest individuals (d = 1.2 mm), c/c_0 hit a low of 0.42 at a mean shear rate of 2.1 s^{-1}. The lowest point for the mid-sized *D. magna* individuals (d = 1.5 mm) was 0.33 at a shear rate of 2.7 s^{-1} and, finally, the experiments done with the biggest *D. magna* individuals (d = 1.8 mm) reached the minimum of 0.18 at a shear rate of 3.4 s^{-1}. In all three cases there was an enhancement in the filtering capacity of *D. magna* at lower shear rates, which lasted longer in the experiments carried out with bigger *D. magna* individuals, and after hitting the peak (corresponding to the

maximum filtering capacity, depending on the body length) there was a fast rise in the values of c/c_0, indicating the entrance into the inhibited filtering regime. For mean shear rates above 6.5

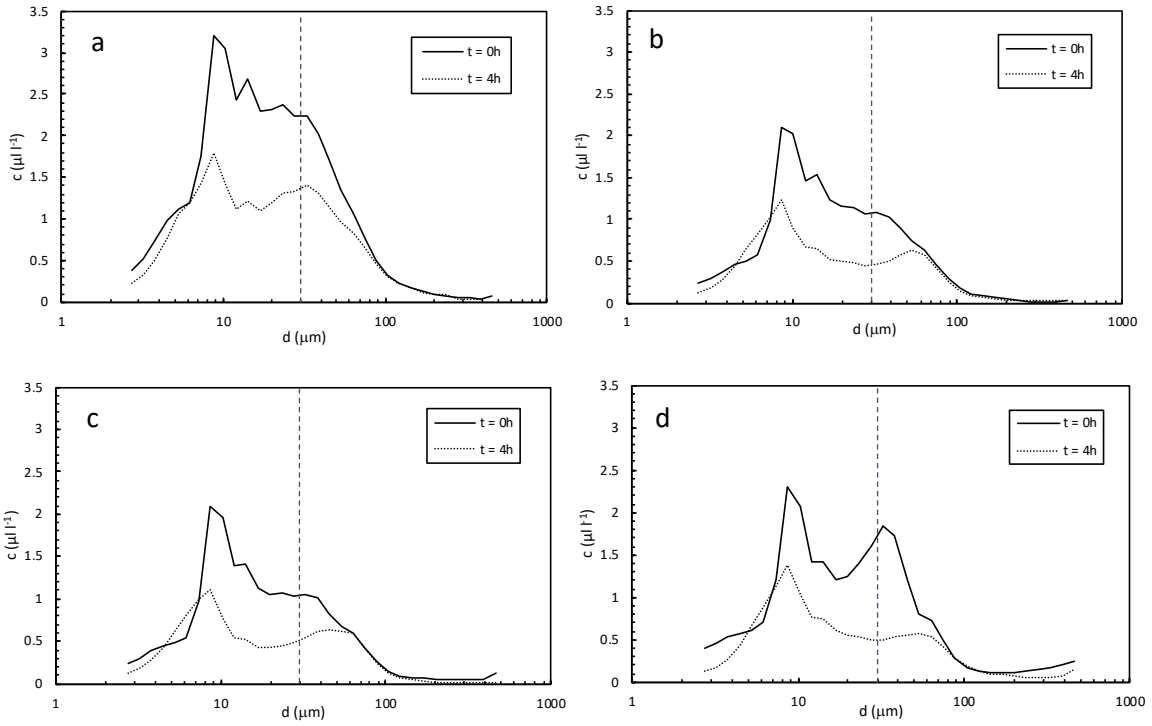

Fig. 7. Particle size distribution for the case of experiments carried out at G = 7.9 s^{-1} for two time steps, initially (t = 0 h) and after 4h of treatment (t = 4 h). (a) corresponds to the control experiment carried out without *D. magna* individuals and (b), (c) and (d) correspond to the experiments carried out with *D. magna* individuals with body lengths of 1.2, 1.5 and 1.8 mm, respectively. The dashed vertical line corresponds to the limit of the ingestion particle size by *D. magna* individuals. In the vertical axis, the particle volume concentration in µl l^{-1} is represented and in the x-axis the diameter of the suspended particles in µm with logarithmic scale. Samples were diluted with bottled mineral water with a dilution factor of 1:1.

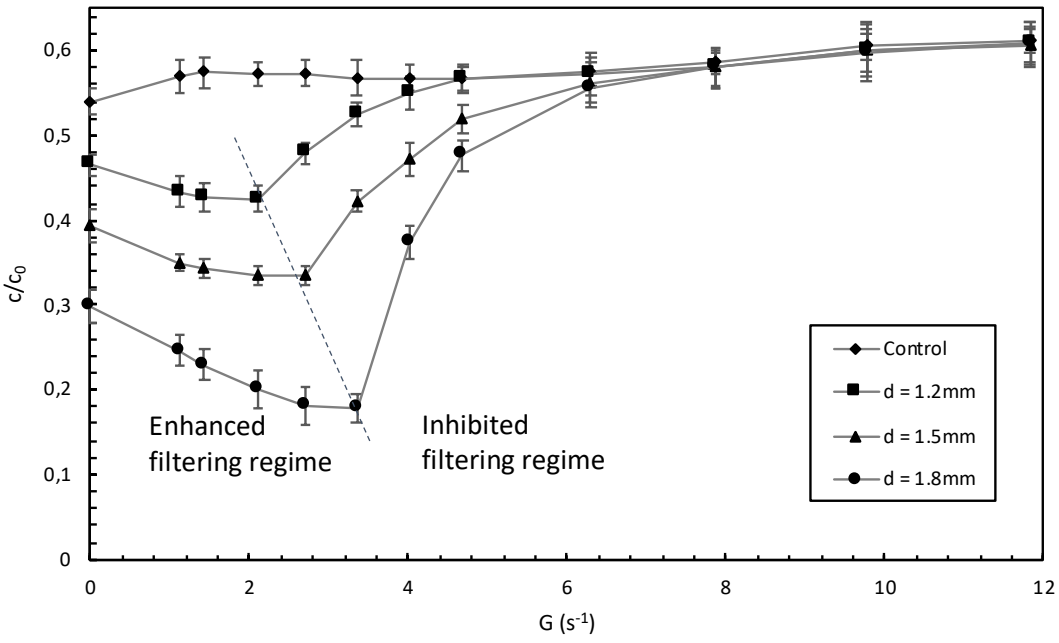

Fig. 8. Ratio of the particle volume concentration (c/c_0) versus the mean shear rate (G in s^{-1}) for the runs with and without *D. magna* individuals. The experiments with *D. magna* were carried out for three different *D. magna* lengths (d = 1.2, 1.5 and 1.8 mm). The dashed line corresponds to the change in filtering regimes.

s^{-1}, the c/c_0 values were the same as that obtained for the control experiments without *D. magna*. The shear rates of the enhanced filtering regime coincided almost completely with those obtained for the laminar flow regime of the Couette flow by Serra et al. (2018), while the mean shear rate of the inhibited filtering regime corresponded to their turbulent flow regime, with c/c_0 values above those at steady flow conditions and equal to those obtained without *D. magna* individuals.

5.3. *D. magna* filtering capacity

The filtering capacity (F) of *D. magna* for each experiment and each mean body length in the zero mean flow was calculated with Eqs. (13) and (14) and is represented in Fig. 9. The filtration capacity at rest was 0.75 ml ind^{-1} h^{-1} for individuals with a mean body length of 1.2 mm, 1.59 ml ind^{-1} h^{-1} for a mean body length of 1.5 mm and 2.97 ml ind^{-1} h^{-1} for a mean *D. magna* size of 1.8 mm. After these values, F increased significantly up to 1.48 ml ind^{-1} h^{-1} (d = 1.2 mm), 2.69 ml ind^{-1} h^{-1} (d = 1.5 mm) and 5.83 ml ind^{-1} h^{-1} (d = 1.8 mm) and then dropped abruptly when turning from the enhanced filtering regime into the inhibited filtering regime, reaching values nearly constant and equal to 0 ml ind^{-1} h^{-1}.

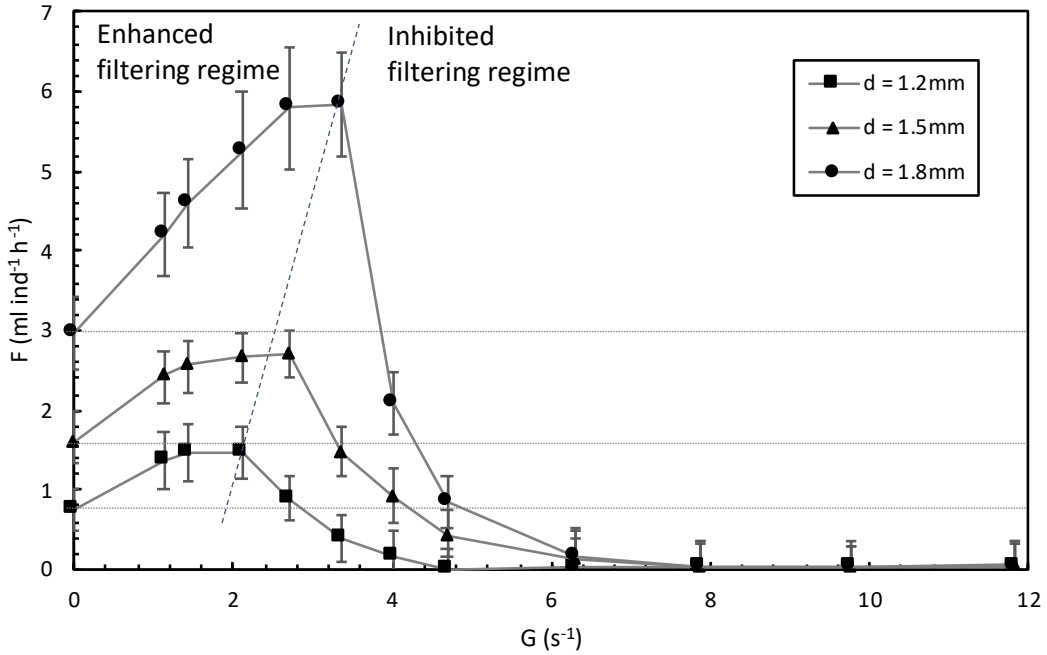

Fig. 9. Filtration capacity of *D. magna* individuals (in ml ind^{-1} h^{-1}) versus the mean shear rate (in s^{-1}) for the runs with and without *D. magna* individuals. The experiments with *D. magna* were carried out for three different *D. magna* lengths (d = 1.2, 1.5 and 1.8 mm). The dashed line corresponds to the change in filtering regimes. The horizontal lines correspond to the *D. magna* filtration in quiescent flow, depending on the body length.

Burns (1969a, 1969b) found that the filtration rate (F) of *D. magna* depended positively on the body length (L) with a power dependence of 2.8 when the water temperature was 20 °C. Moreover, Serra et al. (2018) found that when including the shear rate (G), there was a power relationship of 3 between F and L, similar to that found by Burns (1969a, 1969b). However, Serra et al. (2018) only included one *D. magna* size, which was considered of the same order as the Kolmogorov length scale. In contrast, in this study three different *D. magna* body lengths were evaluated (d = 1.2, 1.5 and 1.8 mm) and the Kolmogorov scale calculated was situated slightly above these values. Hereafter, it was found that the F and the L values obtained for the different experiments followed a power relationship of 2.3 instead of 3. Then, according to Eq. (20) and with the α value obtained by dividing the experimental F values by the theoretical F values, represented in Fig. 10, the *D. magna* filtration can be written as

$$F = 0.08G^{2/3}L^{7/3} + F(0)$$

where F(0) = 0.208 μl ind^{-1} s^{-1} for a mean body length of 1.2 mm, F(0) = 0.443 μl ind^{-1} s^{-1} for a mean body length of 1.5 mm and F(0) = 0.824 μl ind^{-1} s^{-1} for a mean body length of 1.8 mm.

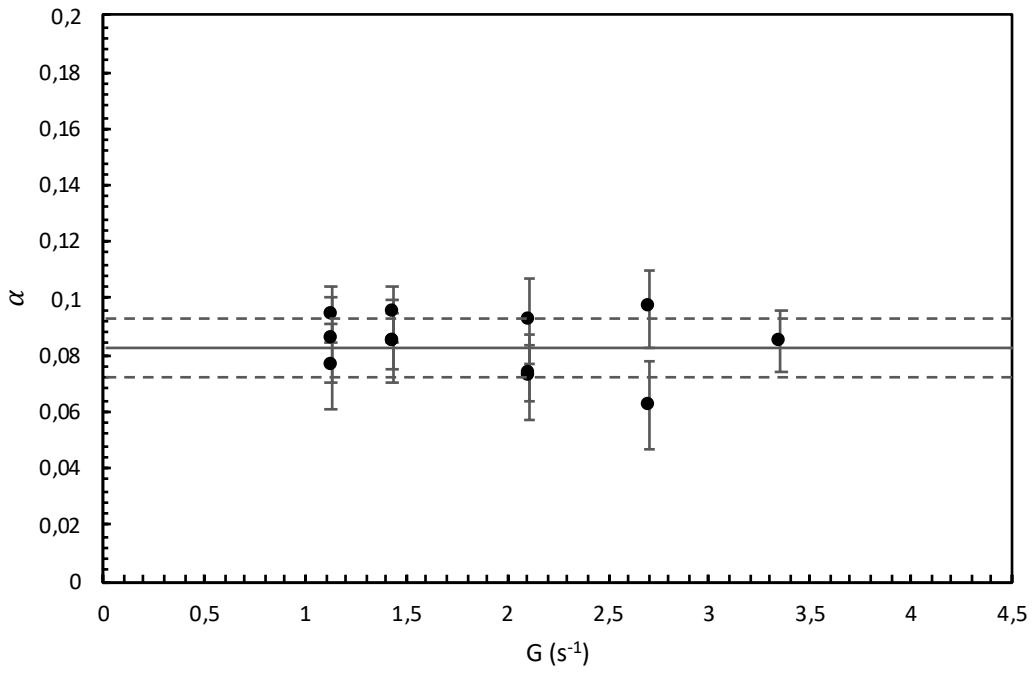

Fig. 10. Capture efficiency (α) versus the mean shear rate (G, in s^{-1}). The continuous horizontal line corresponds to the average α value and the two dashed lines correspond to the standard deviation.

5.4. *D. magna* survival

The 24h-survival of the *D. magna* individuals with three different body lengths (L = 1.2, 1.5 and 1.8 mm) versus the shear rate is plotted in Fig. 11. At lower shear rates (0 – 3.35 s^{-1}), the survival of the largest *D. magna* individuals (L = 1.8 mm) was greater, due to their higher filtration capacity. In contrast, smaller individuals were less resistant to the water flow and therefore less capable of swimming freely and filtering properly, presenting higher mortality. However, between shear rates of 3.35 s^{-1} and 4.01 s^{-1} there was a change in the trend, that is, the larger individuals presented higher mortality than the smaller ones. The shear rates responsible for the changing trend in the survival of *D. magna* individuals match with the transition from laminar to turbulent flow obtained by Serra et al. (2018) for the Couette flow.

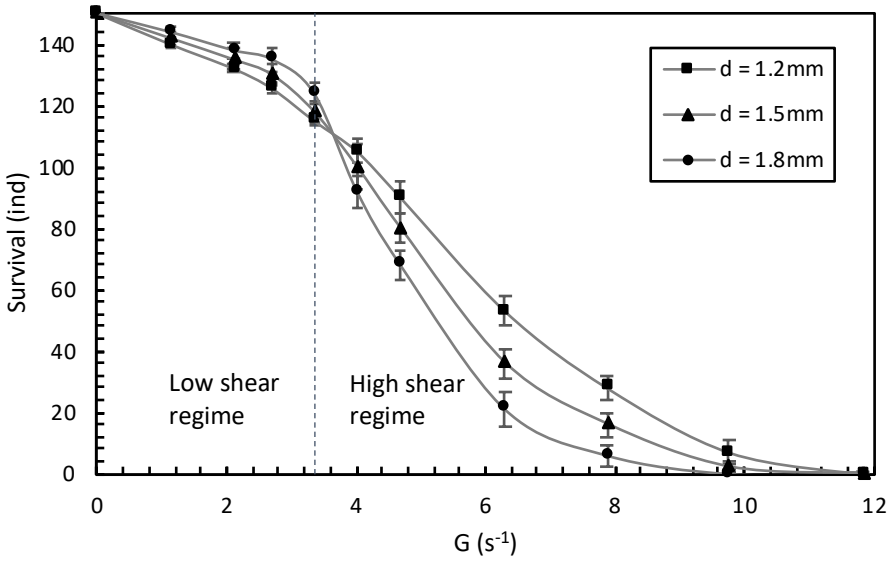

Fig. 11. Survival of *D. magna* individuals for three different body lengths (d = 1.2, 1.5 and 1.8 mm) versus the shear rate (G, in s^{-1}). The dashed line represents the transition from the low shear regime to the high shear regime.

6. DISCUSSION

Zero mean turbulence clearly has a significant effect on the filtering capacity, the mobility and the 24h-survival of *D. magna* individuals. Low mean shear rates enhance filtration efficiency of *D. magna* and allow individuals to control their mobility, whilst high mean shear rates inhibit *D. magna* filtration as well as their capacity of swimming freely, thus causing high mortality rates.

The filtration capacity of *D. magna* individuals with mean body lengths of 1.2, 1.5 and 1.8 mm in quiescent flow was 0.75, 1.59 and 2.97 ml ind^{-1} h^{-1}, respectively. The significant increase in

the filtration capacity obtained at low shear rates is similar to that obtained by Serra et al. (2018) for *D. magna* individuals with a mean body length of 1.6 mm under laminar flow conditions. Likewise, this enhancement in the particle removal is attributed to the increase in the particle-*Daphnia* encountering frequency. However, this positive relation was only found at low shear rates. After reaching a peak of 1.48, 2.69 and 5.83 ml ind^{-1} h^{-1} for individuals 1.2, 1.5 and 1.8 mm long, respectively, there was a sharp decrease in the filtration capacity of *D. magna* when increasing the shear rate, until reaching constant filtration values of nearly 0 ml ind^{-1} h^{-1}. The transition from the enhanced filtering regime into the inhibited filtering regime depended on the body length, appearing earlier with smaller individuals. Hereafter, even though high shear rates increase the particle-*Daphnia* encountering frequency, such conditions probably reduce the time available for a *D. magna* individual to capture particles (Lewis and Pedley, 2001; MacKenzie et al., 1994) with greater effect on small individuals, because of their inability to resist the flow. Moreover, Alcarez et al. (1994) found that a turbulence level of 5×10^{-6} m^2 s^{-3} caused an enhancement of the heart beat rate by 14.3% in *Daphnia pulex*, resulting in an increase in the development, excretion and feeding rates. This turbulence level coincided with the interval where the feeding rate was maximized in our study, situated between 4.3×10^{-6} and 7.1×10^{-6} m^2 s^{-3} for the smaller sizes of *D. magna* (d = 1.2 and d = 1.5), whose body lengths were of the same order as the smaller species *D. pulex*.

Even though all the experiments were carried out under turbulent conditions, the shear rates promoting a decrease in the *D. magna* filtration efficiency coincided with the transition from laminar to turbulent flow conditions described by Hinze (1975) and obtained by Serra et al. (2018). Burns (1969a, 1969b) found that the filtration rate of *D. magna* was related to the body length, with a power dependence of 2.8 at 20 °C. Moreover, Serra et al. (2018) achieved the same conclusion, although they found the power dependence to be 3. In this study, filtration values, F, were found to be related to the body length, L, with a power relationship of 2.3 and with a collision frequency, α = 0.08. A similar collision frequency was obtained by Li and Logan (1997) between fractal aggregates and small particles under turbulent shear conditions, where α = 0.09. Moreover, Kobayashi et al. (2004) found that the capture efficiency could reach maximal values of $\alpha \approx 0.5$, although particles with low affinity presented α values close to 0.1. Therefore, a capture efficiency of ≈ 10% could be representative of the *D. magna* ingestion rate, given the fact that it is not an inert particle, but a moving organism that can only capture those particles colliding near to the oral cavity.

The change from the enhanced filtering regime into the inhibited filtering regime coincided with the change in the *D. magna* swimming velocity. Initially, at low shear rates, the *D. magna* individuals were capable of resisting the flow and swimming more or less freely, thus taking advantage of the flow environment and increasing the particle ingestion rate. This phase lasted longer for the biggest individuals (d = 1.8 mm), since they present higher resistance. However, there came a point when the shear rate was too high to be overcome by any *D. magna* individual, so that they were completely dragged by the flow and unable to continue feeding. When analysing the influence of the shear rate, G, and the body length, L, on the swimming velocity for the two regimes the results showed that there were clear differences. At low shear rates, there was a positive influence of G with a power dependence of 0.36, while L had a negative impact with a power of -0.28. Thus, at low G values the shear rate promoted an increase in the average *D. magna* speed, although they were still capable of resisting the flow, especially with greater L values. In contrast, at high shear rates the body length had no longer influence on the mean swimming velocity, since all *D. magna* individuals were dragged by the flow depending only on G, with a power dependence of 0.5.

The relation of both the filtration capacity and the swimming velocity resulted in the survival of the *D. magna* individuals. At low shear rates, *D. magna* individuals were able to overcome the flow and feed successfully, thus presenting low death rates. In contrast, high shear rates inhibited the *D. magna* filtration and their capacity to swim freely, hence increasing mortality. However, at low shear rates, small individuals (d = 1.2) presented less survival than bigger ones, since they were more easily dragged by the flow. Moreover, as the shear rate increased, there came a point where the trend was reversed, that is, bigger individuals presented higher mortality than smaller ones. This change in the survival might be associated with the greater impact of high shear rate turbulence on the bigger *D. magna* individuals, due to their greater volume.

The experimental data obtained during this study clearly follows a canonical model where filtration capacity, F, depends on shear, G, and characteristic length scale, L, of the *D. magna* individuals. The model proves a dependence of F on G and L with a power relation of 0.67 and 2.33, respectively. When adjusting this model to the experimental data, it was possible to obtain the collision efficiency, α, equal to 0.08, indicating that approximately a 10% of the collisions between *Daphnia* and feeding particles result in a proper ingestion.

6.1. Ethics and sustainability

During the whole study ethical and sustainability criteria have been taken into account. The *D. magna* individuals were kept in appropriate conditions of light, oxygen, temperature and water quality and were regularly fed. Although at higher frequencies (*f)* the mortality increased, the methodology was organized so that these deaths were minimized. To do so, the experiments were started at the lowest *f* and were stopped at the *f* with maximum death, without going any further. Plus, the *D. magna* concentration used for the experiments was 50 ind l^{-1}, which is the minimum concentration needed for ensuring enough particle removal efficiency (about 30%) (Pau et al., 2013; Serra and Colomer, 2016). Moreover, the exact amount of bottled mineral water needed to do the experiments was calculated, so as not to waste any of it. Even though the volume of water needed was considerably high, the aim of this study is clearly worth it, as it is intended to reduce water scarcity by taking advantage of wastewater.

7. CONCLUSION

The presence of zero mean turbulence was found to have a significant effect on the filtering capacity, the swimming velocity and the 24h-survival of *Daphnia magna* individuals. At low shear rates, *D. magna* individuals were capable of resisting the flow and taking advantage of it, thus increasing the filtration rate. In contrast, at high shear rates *D. magna* individuals were unable to overcome the flow and the filtration capacity decreased, thus increasing mortality.

The maximum filtration rate at the low shear rate domain was 1.48, 2.69 and 5.83 ml ind^{-1} h^{-1} for individuals 1.2, 1.5 and 1.8 mm long, respectively. These filtration values were 97, 69 and 96% greater than those obtained in quiescent flow, respectively. The results show that there might be an enhancement in the filtration capacity at low shear rates due to the increase in the encountering rate between *D. magna* individuals and suspended particles. However, at high shear rates *D. magna* individuals were unable to capture the particles successfully, thus inhibiting completely the filtration capacity. The experimental data obtained for the filtration rate clearly adjusted to a canonical model where the filtration rate, F, was found to depend on the shear rate, G, and the body length, L, with a collision efficiency, α, of 0.08, indicating that less than a 10% of the collisions between *Daphnia* and feeding particles result in a proper ingestion.

Moreover, at low shear rates the mean swimming velocity of *D. magna* individuals depended on G and L, with a power relationship of 0.36 and -0.28, respectively, as bigger individuals were able to resist the flow and reduce the average swimming speed. In the high shear rate domain, though, the swimming velocity no longer depended on L, since all *D. magna* individuals were dragged by the flow, presenting similar mean swimming speeds.

Both the reduction in the filtering capacity and the swimming control resulted in an increased mortality of *D. magna* individuals. However, small *D. magna* individuals presented lower survival rates at low shears than the bigger ones, showing to be more sensitive to the flow environment. In contrast, when the shear rate increased, bigger *D. magna* individuals turned out to be the more disadvantaged, since their greater volume made them more vulnerable to higher turbulence.

The results obtained in this study provide information on the influence of zero mean turbulence on the filtration capacity and survival of *D. magna* individuals and indicate the appropriate turbulent shear rate for obtaining the maximum efficiency for a tertiary treatment system based on *D. magna* filtration.

8. AKNOWLEDMENTS

This work was supported by the University of Girona funding MPCUdG2016 and by the INNOQUA project from the European Union's Horizon 2020 research and innovation program (Ares (2016) 1770486).

Personally, I would like to thank Dr. Jordi Colomer, the tutor of my thesis, and Dr. Teresa Serra, my tutor of the Degree, both of the environmental physics department of the University of Girona, for constantly helping and supporting me; my family and friends for always believing in me; and Marc Fernádez, my lab mate, for making the working time more entertaining.

9. REFERENCES

Alcarez, M., Saiz, E., Calbet, A., 1994. Small-scale turbulence and zooplankton metabolism: Effects of turbulence on heartbeat rates of planktonic crustaceans. Notes Limnol. Ocean. 39, 1465–1470.

Altshuler, I., Demiri, B., Xu, S., Constantin, A., Yan, N.D., Cristescu, M.E., 2011. An Integrated Multi-Disciplinary Approach for Studying Multiple Stressors in Freshwater Ecosystems: Daphnia as a Model Organism. Integr. Comp. Biol. 51, 623–633. https://doi.org/10.1093/icb/icr103

Bownik, A., 2017. Daphnia swimming behaviour as a biomarker in toxicity assessment: A review. Sci. Total Environ. 601–602, 194–205. https://doi.org/10.1016/j.scitotenv.2017.05.199

Burns, C.W., 1969a. The relationship between body size of filterfeeding cladocera and the maximum size of particle ingested. Limnol. Oceanogr. Lett. 14, 675–678.

Burns, C.W., 1969b. Relation between filtering rate, temperature, and body size in four species of Daphnia. Limnol. Oceanogr. Lett. 14, 693–700.

Colomer, J., Peters, F., Marrasé, C., 2005. Experimental analysis of coagulation of particles under low-shear flow. Water Res. 39, 2994–3000. https://doi.org/10.1016/J.WATRES.2005.04.076

De Silva, I.P.D., Fernando, H.J.S., 1994. Oscillating grids as a source of nearly isotropic turbulence. Phys. Fluids 6, 2455–2464. https://doi.org/10.1063/1.868193

Garcia-Rodríguez, A., Matamoros, V., Fontàs, C., Salvadó, V., 2014. The ability of biologically based wastewater treatment systems to remove emerging organic contaminants--a review. Environ. Sci. Pollut. Res. Int. 21, 11708–11728. https://doi.org/10.1007/s11356-013-2448-5

Garreta-Lara, E., Campos, B., Barata, C., Lacorte, S., Tauler, R., 2018. Combined effects of salinity, temperature and hypoxia on Daphnia magna metabolism. Sci. Total Environ. 610–611, 602–612. https://doi.org/10.1016/j.scitotenv.2017.05.190

Gómez, M., Plaza, F., Garralón, G., Pérez, J., Gómez, M.A., 2010. Comparative analysis of macrofiltration processes used as pre-treatment for municipal wastewater reuse. Desalination 255, 72–77. https://doi.org/10.1016/j.desal.2010.01.014

Grant, S.B., Saphores, J.-D., Feldman, D.L., Hamilton, A.J., Fletcher, T.D., Cook, P.L.M., Stewardson, M., Sanders, B.F., Levin, L.A., Ambrose, R.F., Deletic, A., Brown, R., Jiang, S.C., Rosso, D., Cooper, W.J., Marusic, I., 2012. Taking the 'waste' out of 'wastewater' for human water security and ecosystem sustainability. Science 337, 681–6. https://doi.org/10.1126/science.1216852

Guadayol, Ò., Peters, F., Stiansen, J.E., Marrasé, C., Lohrmann, A., 2009. Evaluation of oscillating grids and orbital shakers as means to generate isotropic and homogeneous small-scale turbulence in laboratory enclosures commonly used in plankton studies. Limnol. Oceanogr. 7, 287–303.

Hinze, J.O., 1975. Turbulence. McGraw-Hill.

Hopfinger, E.J., Toly, J.-A., 1976. Spatially decaying turbulence and its relation to mixing across density interfaces. J. Fluid Mech. 78, 155. https://doi.org/10.1017/S0022112076002371

Huntley, M.E., Zhou, M., 2004. Influence of animals on turbulence in the sea. Mar. Ecol. Prog. Ser. 273, 65–79.

Huppert, H.E., Turner, J.S., Hallworth, M.A., 1995. Sedimentation and entrainment in dense layers of suspended particles by an oscillating grid. Fluid Mech. 289, 263–293.

Kiørboe, T., Saiz, E., 1995. Planktivorous feeding in calm and turbulent environments, with emphasis on copepods. Mar. Ecol. Prog. Ser. 122, 135–145.

Kobayashi, M., Maekita, T., Adachi, Y., Sasaki, H., 2004. Colloid stability and coagulation rate of

polystyrene latex particles in a turbulent flow. Int. J. Miner. Process. 73, 177–181. https://doi.org/10.1016/S0301-7516(03)00072-3
Ku, H.H., 1966. Notes on the use of propagation of error formulas. J. Res. Natl. Bur. Stand. 70C, 263. https://doi.org/10.6028/jres.070C.025
Kunze, E., 2011. Fluid mixing by swimming organisms in the low-Reynolds-number limit. J. Mar. Res. 69, 591–601.
Levine, A.D., Asano, T., 2004. Recovering sustainable water from wastewater. Environ. Sci. Technol. 38, 201A–208A. https://doi.org/10.1021/es040504n
Lewis, D.M., Pedley, T.J., 2001. The Influence of Turbulence on Plankton Predation Strategies. J. Theor. Biol. 210, 347–365. https://doi.org/10.1006/JTBI.2001.2310
Li, X., Logan, B.E., 1997. Collision Frequencies between Fractal Aggregates and Small Particles in a Turbulently Sheared Fluid. Environ. Sci. Technol. 31, 1237–1242. https://doi.org/10.1021/ES960772O
Maceda-Veiga, A., Webster, G., Canals, O., Salvad O, H., Weightman, A.J., Cable, J., 2015. Chronic effects of temperature and nitrate pollution on Daphnia magna: Is this cladoceran suitable for widespread use as a tertiary treatment? https://doi.org/10.1016/j.watres.2015.06.036
MacKenzie, B.R., Miller, T.J., Cyr, S., Leggett, W.C., 1994. Evidence for a dome-shaped relationship between turbulence and larval fish ingestion rates. Limnol. Oceanogr. 39, 1790–1799. https://doi.org/10.4319/lo.1994.39.8.1790
Matamoros, V., Salvadó, V., 2012. Evaluation of the seasonal performance of a water reclamation pond-constructed wetland system for removing emerging contaminants. Chemosphere 86, 111–117. https://doi.org/10.1016/j.chemosphere.2011.09.020
Mekonnen, M.M., Hoekstra, A.Y., 2016. Four Billion People Experience Water Scarcity. Sci. Adv. 2, 1–7. https://doi.org/10.1126/sciadv.1500323
Moison, M., Schmitt, F.G., Souissi, S., 2012. Effect of temperature on Temora longicornis swimming behaviour: Illustration of seasonal effects in a temperate ecosystem. Aquat. Biol. 16, 149–162. https://doi.org/10.3354/ab00438
Orlins, J.J., Gulliver, J.S., 2003. Turbulence quantification and sediment resuspension in an oscillating grid chamber. Exp. Fluids 34, 662–677. https://doi.org/10.1007/s00348-003-0595-z
Pan, Y., Yan, S.-W., Li, R.-Z., Hu, Y.-W., Chang, X.-X., 2016. Lethal/sublethal responses of Daphnia magna to acute norfloxacin contamination and changes in phytoplankton-zooplankton interactions induced by this antibiotic. https://doi.org/10.1038/srep40385
Pau, C., Serra, T., Colomer, J., Casamitjana, X., Sala, L., Kampf, R., 2013. Filtering capacity of Daphnia magna on sludge particles in treated wastewater. Water Res. 47, 181–186. https://doi.org/10.1016/j.watres.2012.09.047
Peters, F., Gross, T., 1994. Increased grazing rates of microplankton in response to small-scale turbulence. Mar. Ecol. Prog. Ser. 115, 299–307.
Pujol, D., Colomer, J., Serra, T., Casamitjana, X., 2010. Effect of submerged aquatic vegetation on turbulence induced by an oscillating grid. Cont. Shelf Res. 30, 1019–1029. https://doi.org/10.1016/J.CSR.2010.02.014
Rehse, S., Kloas, W., Zarfl, C., 2016. Short-term exposure with high concentrations of pristine microplastic particles leads to immobilisation of Daphnia magna. https://doi.org/10.1016/j.chemosphere.2016.02.133
Rouse, P.H., Dodu, E.J., 1955. Diffusion turbulente à travers une discontinuité de densité. La Houille Blanche 4, 522–532. https://doi.org/10.1051/lhb/1955050
Serra, T., Barcelona, A., Soler, M., Colomer, J., 2018. Daphnia magna filtration efficiency and mobility in laminar to turbulent flows. Sci. Total Environ. 621, 626–633. https://doi.org/10.1016/J.SCITOTENV.2017.11.264
Serra, T., Casamitjana, X., Colomer, J., Granata, T.C., 2002a. Observations of the Particle Size Distribution and Concentration in a Coastal System using an In Situ Laser Analyzer. Mar.

Technol. Soc. J. 36, 59–69. https://doi.org/10.4031/002533202787914304
Serra, T., Colomer, J., 2016. The hydraulic retention time on the particle removal efficiency by Daphnia magna filtration on treated wastewater. Int. J. Environ. Sci. Technol. 13, 1433–1442. https://doi.org/10.1007/s13762-016-0985-4
Serra, T., Colomer, J., Baserba, C., Soler, M., Casamitjana, X., 2002b. Quantified distribution of diatoms during the stratified period of Boadella reservoir. Hydrobiologia 489, 235–244.
Serra, T., Colomer, J., Cristina, X.P., Vila, X., Arellano, J.B., Casamitjana, X., 2001. Evaluation of Laser In Situ Scattering Instrument for Measuring Concentration of Phytoplankton, Purple Sulfur Bacteria, and Suspended Inorganic Sediments in Lakes. J. Environ. Eng. 127, 1023–1030. https://doi.org/10.1061/(ASCE)0733-9372(2001)127:11(1023)
Serra, T., Colomer, J., Logan, B.E., 2008. Efficiency of different shear devices on flocculation. Water Res. 42, 1113–1121. https://doi.org/10.1016/J.WATRES.2007.08.027
Serra, T., Colomer, J., Pau, C., Marín, M., Sala, L., 2014. Tertiary treatment for wastewater reuse based on the Daphnia magna filtration – comparison with conventional tertiary treatments. Water Sci. Technol. 70, 705. https://doi.org/10.2166/wst.2014.284
Shiny, K.J., Remani, K.N., Nirmala, E., Jalaja, T.K., Sasidharan, V.K., 2005. Biotreatment of wastewater using aquatic invertebrates, Daphnia magna and Paramecium caudatum. Bioresour. Technol. 96, 55–58. https://doi.org/10.1016/j.biortech.2004.01.008
Simoncelli, S., Thackeray, S.J., Wain, D.J., 2017. Can small zooplankton mix lakes? Limnol. Oceanogr. Lett. 167–176. https://doi.org/10.1002/lol2.10047
Straile, D., 2002. North Atlantic Oscillation synchronizes food-web interactions in central European lakes. R. Soc. 269, 391–395. https://doi.org/10.1098/rspb.2001.1907
Straile, D., 2000. Meteorological forcing of plankton dynamics in a large and deep continental European lake. Oecologia 122, 44–50. https://doi.org/10.1007/PL00008834
Thompson, S.M., Turner, J.S., 1975. Mixing across an interface due to turbulence generated by an oscillating grid. J. Fluid Mech. 67, 349. https://doi.org/10.1017/S0022112075000341
Vollmer, D., Shaad, K., Souter, N.J., Farrell, T., Dudgeon, D., Sullivan, C.A., Fauconnier, I., MacDonald, G.M., McCartney, M.P., Power, A.G., McNally, A., Andelman, S.J., Capon, T., Devineni, N., Apirumanekul, C., Ng, C.N., Shaw, M.R., Wang, R.Y., Lai, C., Wang, Z., Regan, H.M., 2018. Integrating the social and ecological dimensions of freshwater health. Sci. Total Environ. 627, 1–47. https://doi.org/10.1016/j.scitotenv.2018.01.040
Wickramarathna, L.N., Noss, C., Lorke, A., 2014. Hydrodynamic Trails Produced by Daphnia: Size and Energetics. PLoS One 9, e92383. https://doi.org/10.1371/journal.pone.0092383
Xuequan, E., Hopfinger, E.J., 1986. On mixing across an interface in stably stratified fluid. J. Fluid Mech. 166, 227. https://doi.org/10.1017/S0022112086000125